Rev. IBRACON Estrut. Mater., vol. 16, no. 3, e16306, 2023

IBRACON Structures and Materials Journal
Revista IBRACON de Estruturas e Materiais
ISSN 1983-4195 ismj.org

ORIGINAL ARTICLE

Analysis of size effect in shear transfer mechanisms and size effect suppression by transversal reinforcement – contributions to NBR 6118

Análise de efeito de escala nos mecanismos complementares de resistência ao cisalhamento e sua supressão por reforço transversal – contribuições para a NBR 6118

Igor José Santos Ribeiro[a]
José Renato de Castro Pessôa[b]
Túlio Nogueira Bittencourt[a]
André Teófilo Beck[c]

[a]Universidade de São Paulo – USP, Programa de Pós-graduação em Engenharia Civil, São Paulo, SP, Brasil
[b]Universidade Estadual de Santa Cruz – UESC, Programa de Pós-graduação em Ciência, Inovação, e Modelagem de Materiais, Ilhéus, BA, Brasil
[c]Universidade de São Paulo – USP, Escola de Engenharia de São Carlos, São Carlos, SP, Brasil

Received 20 September 2022
Accepted 25 March 2023

Abstract: Size effects are known to be relevant in the shear transfer mechanisms of quasi-brittle materials like concrete. Bažant proposed an asymptotic approximation between plasticity theory and Linear Elastic Fracture Mechanics (LEFM), showing a proportionality of concrete nominal resistance with $d^{-1/2}$, where d is beam depth. Recently, the long-standing shear transfer mechanism expressions of ACI 318:2014 have been updated (ACI 318:2019), with introduction of a size effect factor. In Brazil, recent publications identified non-conservative trends in predictions of ABNT NBR 6118:2014 for larger beam depths; yet, the Brazilian code never considered size effects because they are suppressed by transverse reinforcement. Considering this background, in this manuscript we make a comprehensive analysis of NBR 6118:2014 shear strength predictions using as a reference the papers of ACI-ASCE DatStb 445-D database. The results exhibit strong tendencies in the model error regarding longitudinal reinforcement and effective depth for beams without transversal reinforcement. A two-step analysis is made herein to describe model errors: first, a nonlinear regression for longitudinal reinforcement is made; second, a linear regression is made for size effect. The reliability analysis corroborates that model error may be reduced by introducing size effect and longitudinal reinforcement factors. Next, for beams with transversal reinforcement, smoother tendencies regarding beam depth are noted, indicating a size effect suppression for the beams depths available in the database. However, as the analysis shows that the higher beam depths concentrate most of the results with unconservative model errors, further studies are necessary to accurately describe how transversal reinforcement suppress the size effect.

Keywords: fracture mechanics, size effect, shear transfer mechanisms, size effect suppression, model error.

Resumo: A relevância do efeito escala é conhecida nos mecanismos de transferência de cisalhamento em materiais quase-frágeis, como o concreto. Bažant propôs uma abordagem assintótica entre a teoria da plasticidade e a Mecânica da Fratura Elástica Linear, exibindo uma proporcionalidade da resistência nominal do concreto com $d^{-1/2}$, sendo d a altura útil da viga. Recentemente, a expressão do código norte americano ACI 318:2014 para os mecanismos complementares de cisalhamento foi atualizada (ACI 318:2019), com a inserção de um fator de efeito de escala. No Brasil, publicações recentes identificaram tendências não conservadoras nas previsões da NBR 6118:2014 para maiores valores de d; ainda assim, o código brasileiro nunca considerou efeito escala devido à aparente supressão pelo reforço transversal. Considerando esse cenário, esse artigo faz uma análise abrangente das previsões normativas da NBR 6118:2014 para a resistência ao cisalhamento usando como referência os artigos da base de dados ACI-ASCE DatStb 445-D. Os resultados exibem fortes tendências da variável erro de modelo em relação à taxa de reforço longitudinal e altura útil para as vigas sem reforço transversal. Uma análise em duas etapas é efetuada neste trabalho: primeiro, uma

Corresponding author: Igor José Santos Ribeiro. E-mail: igorjsribeiro@usp.br
Financial support: Fundação de Amparo à Pesquisa do Estado da Bahia (FAPESB), Fundação para o Desenvolvimento Tecnológico da Engenharia (FDTE).
Conflict of interest: Nothing to declare.
Data Availability: the data that support the findings of this study are available from the corresponding author, upon reasonable request.

This is an Open Access article distributed under the terms of the Creative Commons Attribution License, which permits unrestricted use, distribution, and reproduction in any medium, provided the original work is properly cited.

regressão não-linear é realizada, em termos da taxa de reforço longitudinal; na sequência, uma regressão linear é realizada para a altura da viga. A análise de confiabilidade estrutural corrobora os resultados apontando que a incorporação dos fatores para efeito escala e taxa de reforço longitudinal leva à redução do erro de modelo. Para vigas com reforço transversal, são observadas tendências mais sutis de variação do erro de modelo com a altura útil da viga. Contudo, a análise mostra que as maiores alturas de viga ainda concentram a maior parte dos resultados para as quais o modelo é não conservador; logo, mais estudos são necessários para descrever precisamente como o reforço transversal suprime o efeito escala.

Palavras-chave: mecânica da fratura, efeito escala, mecanismos complementares de resistência ao cisalhamento, supressão do efeito escala, erro de modelo.

How to cite: I. J. S. Ribeiro, J. R. C. Pessôa, T. N. Bittencourt, and A. T. Beck, "Analysis of size effect in shear transfer mechanisms and size effect suppression by transversal reinforcement – contributions to NBR 6118," *Rev. IBRACON Estrut. Mater.*, vol. 16, no. 3, e16306, 2023, https://doi.org/10.1590/S1983-41952023000300006

1 INTRODUCTION

Use of increasingly larger cross-sections in structural elements, together with catastrophic failures observed in recent years, point to a need to better comprehend size effects in predictions of current design codes. The shear transfer mechanism is one of the crucial design variables which recent studies related to scalability problem, i.e., size effect. Illustrating this, the American Code ACI 318: 2019 [1], included a factor to consider the observed transitional trend between theory of plasticity and Linear Elastic Fracture Mechanics predictions.

For quasi-brittle materials, such as concrete, Bažant and Oh [2] was a pioneer analyzing the effect of increasing the depth dimension on the fracture energy. The author laid the foundations for adjustments, like those made in ACI 318:2019, which included a factor showing a proportionality of concrete nominal resistance with $d^{-1/2}$, where d is beam depth.

Regarding the beams without transverse reinforcement, both code and recent publications show, from the ACI445-D database covering a wide range of depth variation, that more reliable designs may be obtained through Bažant's approach. In addition, it was also found that the slopes of the adjustment curve were correctly predicted according to the type-II size effect law, as well as the divergence from the usual normative values that disregard it [3], [4]. Nevertheless, authors such as Collins et al. [5] state that when a minimum transversal reinforcement is provided, there is no need to consider size effect due to the suppression occurrence.

In Brazil, the shear resistance of complementary mechanism is calculated through expressions that do not consider size effect for reinforced concrete beams, when transversal reinforcement is provided or not. According to results obtained by Kuchma et al. [6] when investigating the previous ACI 318:2014 [7], which has trends like those present in ABNT NBR 6118:2014 [8], ignoring size effects may result in unconservative design for higher beams depths. Therefore, it is important to analyze the Brazilian code to incorporate a size factor as well.

2 FRACTURE MECHANICS AND SIZE EFFECT

2.1 Fracture Mechanics

Fracture mechanics studies the phenomena of crack appearance and propagation in materials, until complete fracture. For this to occur, it is necessary that tensile stresses have sufficient intensity to successively break the bonds between the atoms that make up the crystalline structure, until there is partial or total separation of the material. According to the way this phenomenon occurs, it is possible to divide the materials into three groups: brittle, quasi-brittle and ductile.

Brittle materials undergo a cleavage process, characterized by break of atomic bonds as the crack propagates along specific crystallographic planes, orthogonal to the loading and with little deformation before rupture. In these materials, as soon as the maximum tensile stress (f_t') is reached, continuity is lost. The type of rupture that is linked to quasi-brittle materials, demonstrate the behavior known as strain-softening. This is characterized by the fact that the load gradually decays after f_t' as the deformations increase.

This rupture characterization for the different materials comes from Linear Elastic Fracture Mechanics (LEFM) and Elastic-Plastic Fracture Mechanics (EPFM). While the former describes materials with a small fracture process zone (FPZ), the latter extends to more materials, since it considers plasticity ahead of the crack tip. At the structural level, global aspects, such as carrying capacity or deflections, may be correctly determined only by considering plasticity in the crack propagation until the material complete discontinuity [9].

Observing concrete compressive tests, Hillerborg et al. [10] sought to describe the crack displacement from the analysis of the stress vs deformation curve (σ x ε), from a uniaxial concrete stress test. The authors observed that after the peak load the deformations were predominantly located at the tip of the crack, until the body was completely fractured. Considering this curve as a function of crack width, the fracture energy (G_F) was established as equivalent to the area under the curve.

Planas et al. [11] also define fracture energy as the external energy required for the expansion of one unit of cohesive crack area to occur. Following the authors [11], the characteristic length (l_{ch}), result of Irwin's formulations estimation for the FPZ dimension applied to the cohesive crack, can be expressed by Equation 1:

$$l_{ch} = \left(\frac{K_{IC}}{f_t'}\right)^2 = \frac{E' G_F}{f_t'^2} \tag{1}$$

where K_{IC} is the critical stress intensity factor for mode I, E' is the modulus of elasticity in plane stress. The smaller l_{ch}, the smaller the area of inelastic processes, the more brittle the material will be. Authors such as Hoover et al. [12] attest that l_{ch}, together with G_F, remain necessary to characterize concrete's post peak curve. Values of l_{ch} for an infinite concrete body, where it would be possible to apply LEFM, usually vary between 0.15 to 0.45m, whereas l_{ch} varies from 0.30 to 2 m for a fully developed FPZ. Thus, it is attested that LEFM is not applicable to concrete in the usual dimensions. This conclusion also points that size effect might occur as the beams increase its dimensions.

2.2 Size Effect Law (SEL)

Two types of size effect are described in the literature, within the energetic approach. Type I, or statistical size effect, is usual for simple concrete structures, is caused by stress redistribution, and occurs as a large crack propagates continuously from a small region containing micro-cracks. The location of this finite region will depend on the material's random resistance, i.e., this approach is energetic and statistical [13], [14].

Type II, in turn, which is more common for reinforced concrete structures, occurs when the propagation of a crack in the quasi-brittle material is preceded by a redistribution of stresses, which occurs in the FPZ. In these cases, the size effect is deterministic for structures already weakened by a wide crack with stable growth, or non-negligible notch in relation to the cross section and larger than the FPZ [15], [16].

Figure 1 exhibits Bažant and Oh's [2] observations of nominal shear resistance (ν) and the logarithm of the ratio between beam depth (D) and transitional dimension (D_0). The second parameter was defined initially as an empirical adjustment parameter, plotted as a vertical line. On the upper part, the horizontal line (blue) represents the classical formulations predictions, which had no dependence on size. As the beam depth increases, the FPZ decreases and the LEFM may be used to describe the shear resistance. From that, the author proposed and transitional approach between plasticity theory and LEFM, as represented by the dashed purple line with slope of 1/2 in Figure 1. The size effect law is plotted as the continuous green curve, describing how ν decreases as the depth increases.

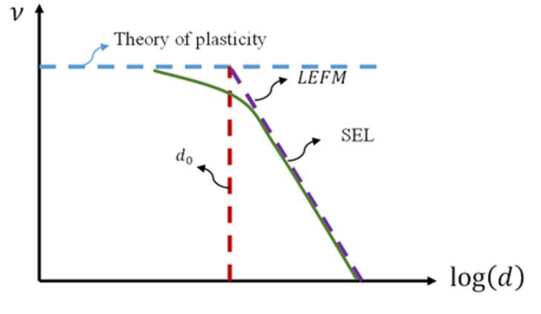

Figure 1 – SEL asymptotic approach: nominal shear strength (ν) in terms of cross-session depth d (log scale).

Hence, the size effect law of Type II (SEL-II) was obtained by making an asymptotic correspondence for geometrically similar structures by varying their depth, as expressed in Equation 2:

$$\nu = \frac{\hat{B} f_t'}{\sqrt{1+\frac{d}{d_0}}} \tag{2}$$

where d is the effective depth, d_0 is the transitional dimension and $\hat{B}$ is defined in the Equation 3:

$$\hat{B} = E' G_f / c_f g'(\alpha_0) \tag{3}$$

where G_f is the initial fracture energy, c_f is the effective length of fracture zone, $g'(\alpha_0)$ is the energy release rate, as function of α_0, the initial crack extension normalized by depth. Later, Bažant and Oh [2] stated that the transitional behavior observed in concrete can be related to the size of FPZ which is not negligible with the increase of member dimensions [16].

3 SHEAR TRANSFER MECHANISMS

3.1 Shear resistance of complementary mechanism parameters

Since the first approaches to analyze shear in concrete structures, several updates were made to insert the discovered shear transfer mechanisms that change the initial truss and tie model predictions. The studies revealed differences due to pin effect, interface friction, cantilever effect, concrete residual tensile strength, among others, and these are considered in the shear resistance codes through a parameter named shear resistance of complementary mechanisms (V_c).

In turn, the current Brazilian code defines expressions based on two models: the fixed angle truss and the variable angle truss. The former has a fixed value for any load, given by:

$$V_c = 0.6 f_{ctd} b_w d \tag{4}$$

where f_{ctd} is the design concrete tensile strength that is calculated by Equation 5:

$$f_{ctd} = \frac{f_{ctk,inf}}{\gamma_c} = \frac{0.7 f_{ctm}}{1.4} = 0.5 f_{ctm} \tag{5}$$

where γ_c is the concrete partial safety factor and f_{ctm} is the mean of concrete tensile resistance calculated according to Equation 6 for concrete with compressive strength up to 50 MPa and Equation 7 from 55 to 90 MPa. The ABNT: NBR 8953:2015 [17] also establishes class C100, which is not covered by the ABNT: NBR 6118:2014 in its current version.

$$f_{ctm} = 0.3 (f_{ck})^{\frac{2}{3}} \tag{6}$$

$$f_{ctm} = 2.11\, ln(1 + 0.11 f_{ck}) \tag{7}$$

The second model starts from the consideration of a truss with variable angle and is divided into different expressions that seek to adjust the load distribution of the classic truss, with possible relief in the struts by reducing the vertical component. This leads to a change in the model for calculating the V_c parameter which, in this approach, depends on the load.

3.2 Size Effect in Shear Resistance of concrete beams

One of the factors that contributes to V_c is the size effect. Different approaches have been made, such as the Canadian standard CSA A23 [18], or the methodology incorporated in the ACI 318:2019 [1], the SEL-II. There is still no consensus on how this should be considered, or even if there is an actual need when the minimum transverse reinforcement is provided [5].

By analyzing geometrically similar structures with different heights, Kani [19] observed that the predicted values for the larger beam depths led to results up to 40% smaller than those predicted by the current formulation.

Based on a probabilistic approach but considering beam depths between 10 and 300cm and distributed loads, Iguro et al. [20] stated that a proportionality of the shear resistance to $d^{-1/4}$ may be considered, to obtain more conservative results.

In the Toronto series, Podgorniak-Stanik [21] considered 7 different beam depths, varying the percentage of longitudinal reinforcement ratio, for specified compressive strength of f_{cr}=37 MPa, and high strength concrete ($f_{cr} = 99\ MPa$), with minimum transverse reinforcement. The author affirmed existence of the size effect, which is more prominent for larger beam depths. Nevertheless, the author [22] also supposed that the stirrups would be sufficient to control cracking. However, according to Bažant et al. [3] it is wrong to infer this from the results. There is a notable reduction for beams reinforced transversally for the considered sizes, although not as significant as for beams without stirrups. The authors also point out that the predictions should be based on the parameter of characteristic compressive strength in the quantile of 9% (f_c'), instead of f_{cr}, and that the curve adjustment should be done at the edge of the dispersion band, instead of in the middle. After comparison with simulations, Bažant et al. [3] concluded that there is a significant reduction due to use of minimal transverse reinforcement, but insufficient for the size effect to become negligible.

Testing beams with effective depths of 300 and 4000 mm, and comparing several proposed predictions, Quach [22] demonstrated that the consideration of the size effect for large sections was necessary for an optimized design. Afterwards, Collins et al. [5], in an article referring to these same specimens, together with the ones from the Toronto series, affirmed an apparent suppression of the size effect based on the more brittle behavior observed. However, this series has maximum value for the beam depth of $d = 1840mm$, insufficient to conclude about a complete size effect suppression. Furthermore, this beam has an $a/d < 2.4$ where the arc action is still the main shear transfer mechanism.

From the database selected by the ACI 445-D committee, Bažant et al. [3] applied an algorithm to randomly eliminate data at intervals to fix the variance of other parameters than beam depth. As their variance affects the size effect, the influence of beam depth become even more notorious after applying Equation 2 to this transformed database, with nominal shear strength proportional to $d^{-1/2}$.

Later, applying the ACI 318 (2014) formulation to the updated database, Yu et al. [4] observed that for small beam depths, the plastic analysis was satisfactory. They also inferred that consideration of a probabilistic approach of the size effect for concrete was not justifiable, given the usual stress redistribution as well as the cracking pattern of the concrete beams under analysis.

3.3 A note on datasets

Different approaches are possible in constructing datasets and subsets. For instance, to reflect advances in materials technology, which are expected to reduce standard deviation, test data could be split into prior and posterior to 1980, as done in [23], [24], [25]. The coefficient of variation per interval depends both on heterogeneity of data and on the formulations. As model predictions are made to all collected data, it is important to consider what goals the authors had when developing the original studies. Due to data heterogeneity, the COV of a larger dataset tends to be larger than that of a smaller dataset.

4 MATERIALS AND EXPERIMENTAL PROGRAM

4.1 Shear test database

4.1.1 Slender beams without transversal reinforcement

Ribeiro et al. [26] analyzed the trends concerning the main complementary mechanisms to shear transfer in ACI 318:2014, ACI 318:2019, Frosch et al. [27] and ABNT NBR 6118:2014 considering slender beams (where the complementary mechanisms have greater influence) from a dataset encompassing 1356 tests available in the ACI-DafStb, filtered as proposed by Reineck et al. [28] and additionally with a f_{ck}>20MPa to select only concrete with structural propose as defined by ABNT NBR 8953:2015.

The results show the most influents mechanisms to the model error and points towards the possible adjust through minimum square regression concerning longitudinal reinforcement ratio and later a linear regression to beam depth. Therefore, we start from the same database focused solely on propose an adjusted model to reduce the previously observed trends.

4.1.2 Slender beams with transversal reinforcement

Size effect suppression with use of stirrups was pointed out by Collins et al. [5], corroborated by Kuchma et al. [6] and opposed by Yu and Bažant [29]. To verify size effect suppression, the database provided by Reineck et al. [30] was employed herein: 886 beams were selected, of which 556 had *a/d* > 2.4.

After applying the filters recommended by Reineck et al. [30], removing beams that suffered rupture other than by shear, as well as spurious or missing data, a set of 170 beams with no axial forces, was obtained. Also, this database is like the one used by the ACI 445-D committee for adequacy. Similarly, a filter was applied for structural concrete, which removed only 6 beams from the sample set. The data taken from 39 authors is reported in Annex A.

4.2 Calculation of shear resistance of complementary mechanisms ($\boldsymbol{V_c}$)

4.2.1 Beams without stirrups

From the ABNT: NBR6118:2014, solely the Model I, previously exposed in Section 3.1 and calculated by Equation 4 was used by Ribeiro et al. [26] because of the available data for calculations.

4.2.2 Beams with stirrups

To verify the size effect suppression, the strength of beams with stirrups is calculated. The formulations by Frosch et al. [27], ACI 318: 2014 [7] and ACI 318: 2019 [1] have the same normative prescription for the transversal reinforcement resistance, for beams where reinforcement is greater than the minimum. The Brazilian formulation is like the *fib* Model Code [31].

4.2.2.1 Approach from ACI 318 and Frosch et al. [27]

Based on the fixed-angle truss model with contribution of complementary mechanisms, the standards prescribe that the strength of a beam with transverse reinforcement will be given by Equation 8:

$$V_n = V_s + V_c \tag{8}$$

For ACI 318:2019, the shear strength of the complementary mechanisms follows the expressions of ACI 318:2014 when at least minimum transversal reinforcement is provided. The transversal reinforcement shear strength is calculated by Equation 9:

$$V_s = \frac{A_{sw}}{s_w} f_{yw} d \tag{9}$$

Substituting the respective expressions, the value of the ultimate shear strength of a beam is calculated by Equation 10:

$$V_u = 0.166\sqrt{f_c'}\, b_w d + \frac{A_{sw}}{s_w} f_{yw} d \tag{10}$$

For the expression by Frosch et al. [27], Equation 11 must be used:

$$V_u = 0.415\,\sqrt{f_c'} b_w c + \frac{A_{sw}}{s_w} f_{yw} d \tag{11}$$

Where c is the depth of the cracked cross-section, calculated by Equation 12:

$$c = kd \tag{12}$$

Where k is a coefficient relating reinforcement and concrete given by Equation 13:

$$k = \sqrt{2\rho_L n + (\rho_L n)^2} - \rho_L n \tag{13}$$

Where ρ_L is the longitudinal reinforcement ratio (%) and n is the ration between reinforcement end elasticity modules.

4.2.2.2 Code NBR 6118 (2014)

Since the Brazilian code also starts from the fixed angle truss model with V_c contribution, Equation 8 will be used. Therefore, for the Brazilian standard, the resistance is calculated by Equation 14:

$$V_u = 0.6 f_{ctd} b_w d + \frac{A_{sw}}{s_w} 0.9 d f_{yw} \tag{14}$$

4.3 Model error

The model for the beams without stirrups in Equation 4 provides one estimate of shear strength (V_c) for each of the beams of the experimental database. Similarly, for beams with stirrups the model in Equations 20-22 provides one estimate of total shear resistance V_u. If V_M is the shear strength predicted by the model (M), and V_E is the shear strength observed in the experiment (E), then observations of a model error variable (ME) can be obtained by Equation 15:

$$ME = \frac{V_E}{V_M} \tag{15}$$

The model error ratio (ME) shows how the predictions are close to the actual tests results. If $ME < 1$, the experimental strength is smaller than the model-predicted strength, potentially leading to an unsafe design. The higher the value of ME, the more conservative is the model prediction. Beck et al. [32] used ME to identify tendencies in circular steel concrete-filled steel columns regarding the slenderness ratio and later applied non-linear regression to describe the relation between parameters.

Based on a statistical analysis of a set of model error observations, statistics like mean (μ_{ME}), standard deviation (σ_{ME}) and coefficient of variation ($\delta_{ME} = \sigma_{ME}/\mu_{ME}$) can be computed. The ideal model should have $\mu_{ME} = 1$ and $\delta_{ME} = 0$, but this is unrealistic due the uncertainties inherent to any model. A good engineering model will have $\mu_{ME} \approx 1$ and δ_{ME} as small as possible. When $\mu_{ME} > 1$ we say that, on average, the model is conservative; but this may not be sufficient if δ_{ME} is large!

In this manuscript, we interpret model error results by reporting the mean (μ_{ME}) and coefficient of variation (δ_{ME}), as well as the percentage of results for which $ME < 1$ (potentially unsafe). Also, we report model error results for two upper fractiles (UF), corresponding to 90 and 95%. These fractiles highlight models that are excessively conservative, when $UF \gg 1$.

5 RESULTS AND DISCUSSIONS

5.1 Application of a size effect factor to ABNT: NBR 6118:2014

There is a strong influence of the size effect, demonstrated with the increase in effective depth. Considering that Barros et al. [33] exhibit trends regarding the minimum longitudinal reinforcement to slabs, Ribeiro et al. [26] to beams, and that this parameter is expected to change with increasing effective depth, a two steps regression is proposed.

First the same dataset in terms of longitudinal reinforcement ratio (ρ_L) is exhibited in Figure 2. For the Brazilian code the model error increases with ρ_L from unconservative design for lightly reinforced beams (ME<1) to excessively conservative design. The tendencies in model error concerning longitudinal reinforcement ratio per range are more detailed in Table 1.

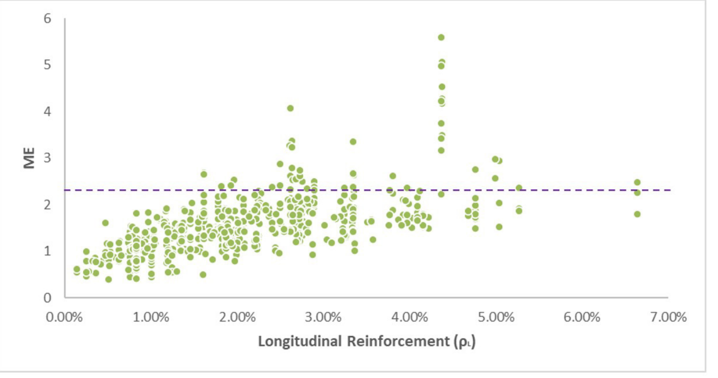

Figure 2 – ME x ρ_L for NBR 6118:2014

Table 1 – ME with respect to longitudinal reinforcement ratio

N	ρ_L (%)	ME <1 (%)	μ_{ME}	δ_{ME}
125	0-1.30	44.0%	1.05	0.32
207	1.30 – 2.60	5.13%	1.54	0.25
149	2.60 – 3.90	0.00%	1.86	0.27
68	3.90 – 6.70	0.00%	2.39	0.42

To correct these tendencies a power function is proposed, similarly to ACI 318:2019, given by Equation 16:

$$V_{c0} = 0.6 f_{ctd} b_w (a\, \rho_L^b) \tag{16}$$

where a and b are parameters of a power function to be determined by regression. By way of minimum squares regression analysis, the following Equation 17 is obtained:

$$V_{c0} = 0.6\, f_{ctd} b_w (8.6 \rho_L^{0.44}) \tag{17}$$

The ACI 318 (2019) uses $\rho_L^{0.33}$, close to the obtained result. Next, the model in Equation 17 is applied to the same database, obtaining new ME results which do not have trends concerning ρ_L as presented in Figure 3. Also, the 90% fractile is $UF = 1.4$ for this correction. After implementing Equation 17, the ME data still exhibits a trend with respect to beam depth, as seen in Figure 4.

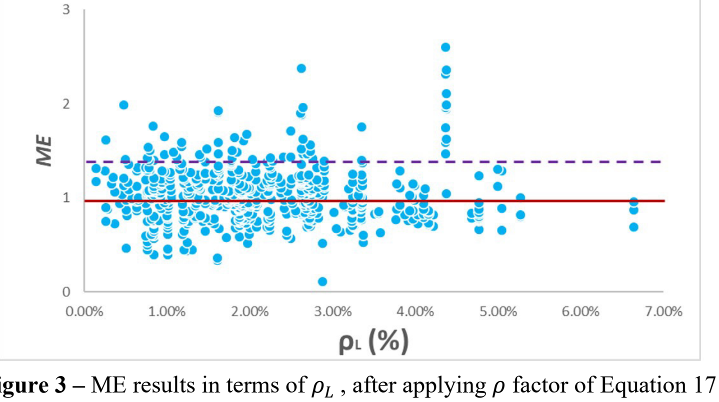

Figure 3 – ME results in terms of ρ_L , after applying ρ factor of Equation 17

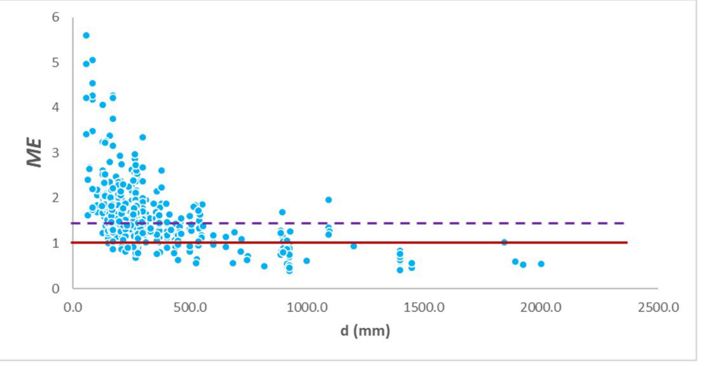

Figure 4 – ME in terms of d after application of ρ_L factor

Therefore, as the size effect law is already defined, a change of variable in d is made to (tentatively) linearize the data in Equation 18:

$$y' = \frac{1}{\sqrt{1+\frac{d}{d_0}}} \tag{18}$$

where $d_0 = 254\ mm$. Once the data is (tentatively) linearized, a linear regression analysis is made on variable y', to determine the coefficient a, of the Equation 19:

$$y = ay' \tag{19}$$

Once determined, it can be used to correct the model as proposed in the size effect factor defined by Equation 20:

$$\gamma_e = \sqrt{\frac{1{,}53}{1+d/d_0}} \tag{20}$$

Applying the model error correction of (Equation 20), the distribution of data points in Figure 5 is obtained. On (a) the ME for ABNT NBR6118:2014 and on (b) for the corrected model.

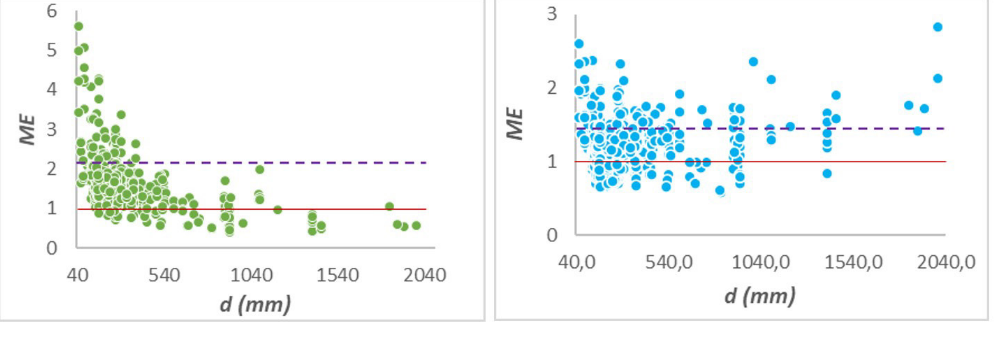

(a) (b)

Figure 5 – ME results for ABNT NBR 6118:2014 without (a) and with (b) ρ_L and γ_e factors.

Clearly, there are no more tendencies in the new proposed design, exhibiting that the proposed equation correctly describes the functional relation among the parameters. The 90% fractile is $UF = 1.60$, indicating a less conservative approach, since the NBR 6118:2014 had $UF = 2.24$. Since the insertion of the factor ρ_L does not foresee that as the beam height increases the pin effect reduce its role in the shear resistance output, this is the most likely cause of the increasing in *ME* for higher beam depths. The final proposed expression, to be adjusted accordingly the desirable safety is given in Equation 21:

$$V_c = 5.2\gamma_e f_{ctd} b_w d \rho_L^{0.44} \tag{21}$$

This expression may be corrected through a reliability analysis establishing a target reliability index.

5.2 Structural Reliability Analysis

To further evaluate the proposed expression the First Order Reliability Method (FORM) was applied to both the proposed expression (18), and the current code. First, same beam depth intervals used in Ribeiro et al. [26] were used. The mean of ME (μ_{ME}) and the coefficient of variation (δ_{ME}) of each range was used to compute the standard deviation by:

$$\sigma = \delta_{ME} \times \mu_{ME} \tag{22}$$

The beam width was considered a deterministic parameter with $b_w = 200mm$. Since size effect takes place to $d > 254mm$ and varies among the intervals, beams depth of 375, 625, 875, and 1500mm were considered.

Since the most of dataset is comprehended between $20 < f_{ck} < 40\ MPa$, compressive strengths of 20, 30 and 40 MPa were used in this analysis as random variables with normal distribution. Finally, to analyze how the longitudinal reinforcement ratio affect the model were used $\rho_{L,min}$, $\rho_{L,m}$ and $\rho_{L,max}$, where $\rho_{L,min}$ correspond to the design code minimum longitudinal reinforcement to the beams in analysis, $\rho_{L,max}$ corresponds to the maximum value observed in dataset and $\rho_{L,m}$ is the median of this parameter. As b_w, d and ρ_L were considered as deterministic variable the resistance in the limit function state depends only on f_c for both the current design code and the proposed.

Regarding the loads, dead load (D) was considered with a normal distribution, live load (L) and wind load (W) as Gumbel Distributions. The load combination was made as the design code NBR 6118:2014 applying the so-called Turkstra combination, considering the maximum of Live Loads (L) for 50 years and the maximum annual wind load (W_1). In turn, for both mean model error of resistance ($E_{M,R}$) and for the loads ($E_{M,S}$), normal distributions were considered. Next, the limit state equations were considered as Equation 23:

$$g\left(f_c, D, L, W_1, E_{m,r}, E_{m,l}\right) = E_{M,R} * R(f_c) - E_{M,S} * S(D + L_{50} + W_1) \tag{23}$$

As aforementioned, $E_{M,R}$ was considered for the same beam depth intervals in Table 2. The $E_{M,S}$ was used accordingly JCSS [34] with mean value of 1.00 to shear and $\delta_{E_{M,S}} = 0.10$ $R\ (f_c)$ is given by Equations 4 and 21, for the Brazilian code and for the proposal, respectively, resulting in Equations 24 and 25:

$$g_1(R, S) = E_{M,R} * 0.6 * \left(0.21 f_c^{\frac{2}{3}}\right) b_w d - E_{M,S} * (D + L_{50} + W_1) \tag{24}$$

$$g_2(R, S) = E_{M,R} * 5.2 * \left(0.21 f_c^{\frac{2}{3}}\right) b_w d * \rho_L^{0.44} - E_{M,S} * (D + L_{50} + W_1) \tag{25}$$

The function g_1, is the limit state function when ABNT NBR 6118:2014 is considered and g_2, when the proposal is used. The Tables 3-4 summarizes the distribution data to resistance and load parameters, respectively, available in Santiago et al. [35] and Costa et al. [36] to live loads.

Table 2- Concrete compressive strength distribution parameters

Random Variable	Compressive Strength Class	Distribution	Mean(μ)	$C.O.V.(\delta)$
f_c	C20	Normal	$1.30f_c$	0.20
	C30	Normal	$1.22f_c$	0.15
	C40	Normal	$1.16f_c$	0.11

Table 3- Loads distribution parameters

Random Variable	Distribution	Mean(μ)	$C.O.V.(\delta)$
D	Normal	$1.06D_n$	0.12
L	Gumbel	$0.92L_n$	0.25
W1	Gumbel	$0.33W_n$	0.47

Where D_n, L_n and W_n refer to nominal values of Dead Load, Live Load and Wind Load, respectively. The Dead Load parameters were taken from Santiago et al. [35]. The Live Load values were taken from Costa et al. [36], who made a comprehensive study of stochastic models for live loads, including comparison to design values of NBR 6120:2019. Finally, the Wind Loads used are based in the results obtained by Beck and Souza [37]. The failure probability may be obtained by:

$$p_f = \int_{g(x)\leq 0} f_x(x)\, dx \tag{26}$$

Where $g(x) \leq 0$ is the failure probability domain, and f_x(x) is the joint probability distribution function of the random variables in this problem. When FORM is applied, the previous equation, and its limits state function described in Equations 25-26, is mapped into a standard gaussian space, and the design point may be found, representing the point over failure domain closest to the standard space origin. Hence, the reliability index (β) may be determined as, precisely, this distance. By solving this problem using FORM, sensitivity coefficients (α) that are used on interpreting the results by identifying the relative contribution of each random variable.

5.2.1 Structural reliability results

The Figure 6 shows the obtained result to C20. The three longitudinal reinforcement ratio used are represented as $r_1 = \rho_{L,min}$, $r_2 = \rho_{L,m}$ and $r_3 = \rho_{L,max}$.

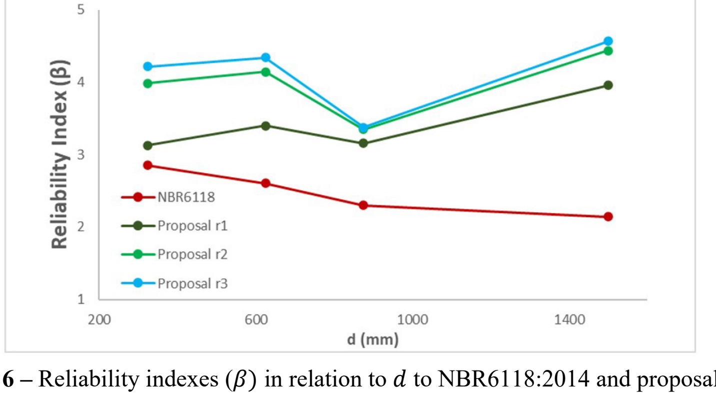

Figure 6 – Reliability indexes (β) in relation to d to NBR6118:2014 and proposal: C20

The Figure exhibit a notorious trend in the NBR 6118:2014 to reduce β as the beam depth increases. On the other hand, the introduction of the correction factors concerning ρ_L and d leads to higher β values to the beams considered. The higher ρ_L is, the higher β becomes. The sensitivity factors to NB 6118 are shown in the Figure 7 and on Figure 8 to Proposal-$r1$ where the model error changes were higher.

Although there is some other small contribution, the Figure 7 shows that for this analysis the model error of resistance variables is the more influent parameter to resistance.

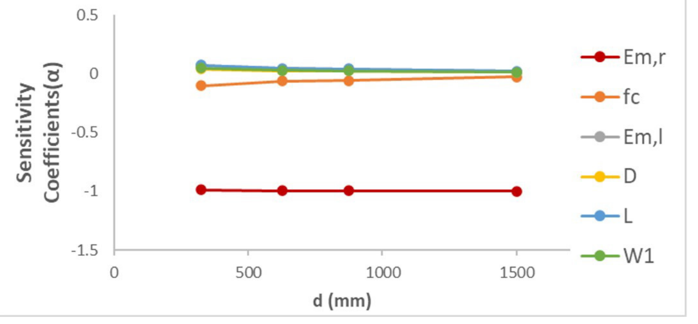

Figure 7 – Sensitivity coefficients to NB6118:2014 to C20

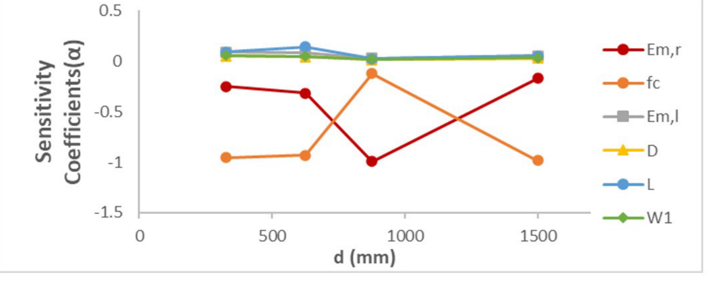

Figure 8 – Sensitivity coefficients to Proposal-r_1 to C20

In turn, the Figure 8 show a significant contribution of this variable in 500-1250mm intervals, indicating the model proposed has a better performance to light reinforced beams. Concerning the loads, the Live Load was the most influent parameter in this analysis until beam depth of 750mm. Considering the Compressive Strength Class C30, the Figure 9 is obtained.

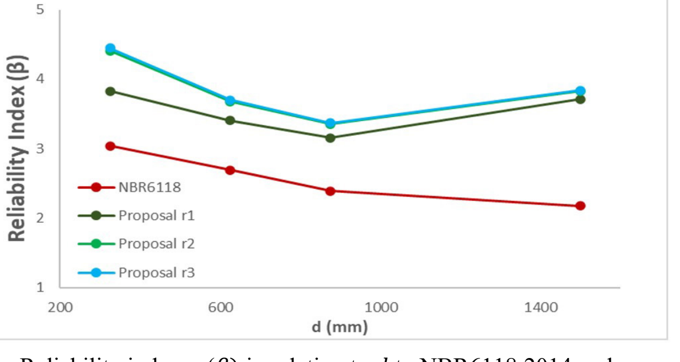

Figure 9 – Reliability indexes (β) in relation to d to NBR6118:2014 and proposal: C30

The reliability index exhibits the same pattern, reducing as the beam depth increases. Similarly, the same trends are obtained to de proposal with slightly higher values for the first considered beam depth.

The sensitivity coefficients from the FORM are show at Figure 10 to NBR 6118:2014 and at Figure 11 to Proposal-$r1$. The tendencies now are similar in Figures 12-13, even though the proposal still holds smaller values to the considered beam depth and higher values to Live loads.

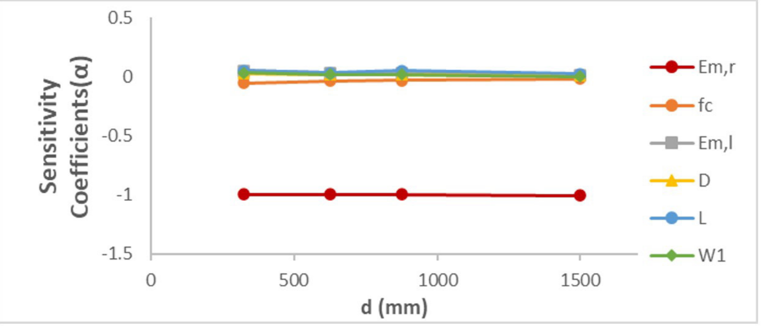

Figure 10 – Sensitivity coefficients to NB6118:2014 to C30

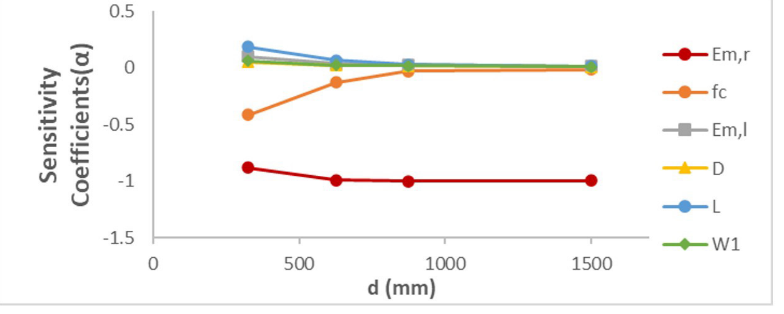

Figure 11 – Sensitivity coefficients to Proposal-$r1$ to C30

This change with concrete compressive strength may be a consequence of considering only compressive resistance as a random variable. Considering C40, the Figure 14 is obtained.

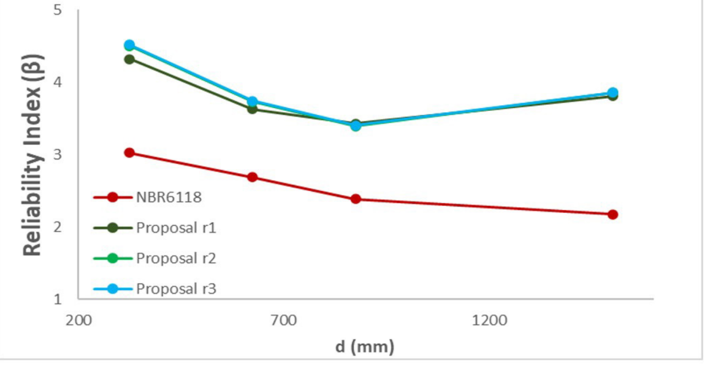

Figure 12 – Reliability indexes (β) in relation to d to NBR6118:2014 and proposal: C40

The NBR 6118:2014 reach lower values to β, but it still holds the same pattern as C20 and C30. Meanwhile the difference between the maximum and the minimum β becomes larger as compressive strength increases.

The sensitivity coefficients to C40 are shown in Figure 13 to NBR 6118 and in Figure 14 to Proposal-r_1. The pattern remains alike both designs and slightly smaller to NBR 6118 (2014). The live loads had greater influence in the current code than the proposed formulation to this concrete class.

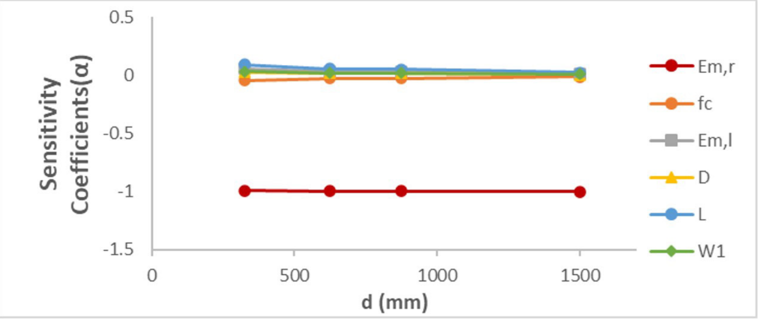

Figure 13 – Sensitivity coefficients to NB6118:2014 to C40

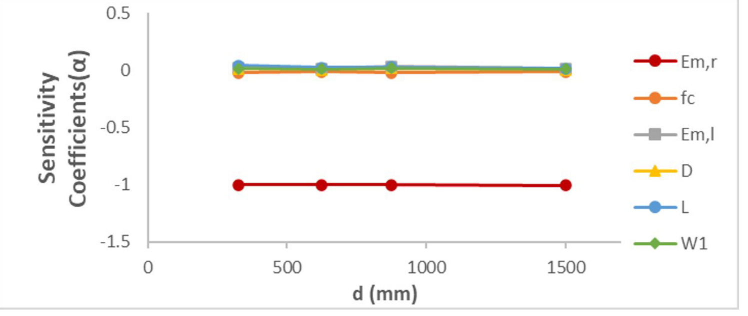

Figure 14 – Sensitivity coefficients to Proposal-$r1$ to C40

5.3 Size effect analysis in beams with transversal reinforcement

From the database for reinforced concrete beams with stirrups, the parameter d distributions in Figure 15 are obtained. For the effective depth, fewer samples higher than 1000 mm are noted, where the formulations under analysis present most of the values for which ME <1.

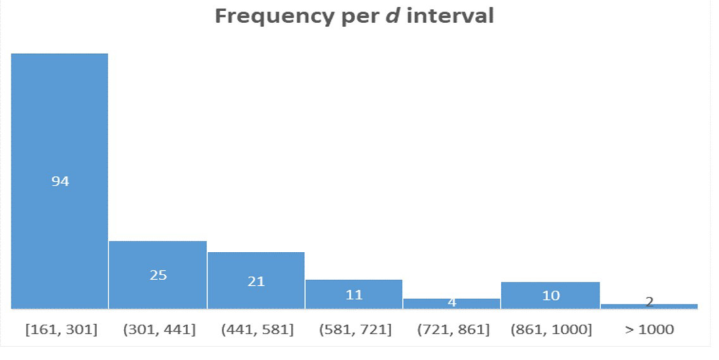

Figure 15 – Effective depth distribution (mm).

Table 4. Model error 90% fractile and percentage of results above fractile, for different beam depths and codes.

	Code	ACI 318 2014	NBR6118 2014	Frosch [27]
	90% ME fractile	1.71	2.10	2.06
N	Beam depth d (mm)	**Fraction of results above the 90% fractile**		
23	0-250	34.78%	13.04%	13.04%
112	250-500	7.21%	12.61%	13.51%
15	500-750	0.00%	0.00%	0.00%
15	750-1300	0.00%	0.00%	0.00%

As observed in Table 3, most of the results above the upper fractile are in the same range where most of the data is, i.e., between zero and 500 mm.

In this dataset, even though the tendencies are smaller, they are still observable only in effective depth in Figure 16, where (a) is ACI 318 (2019), (b) is the NBR 6118 (2014), and (c) is the Frosch [27]. Whenever transversal reinforcement is provided the ACI 318:2014 remains in the newest code version (ACI 318:2019).

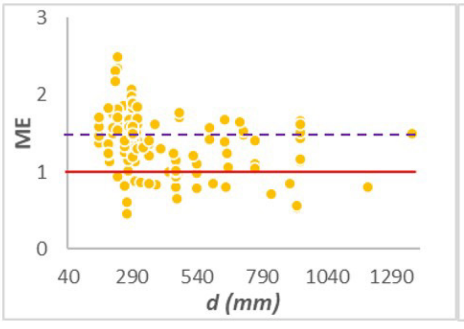

(a)

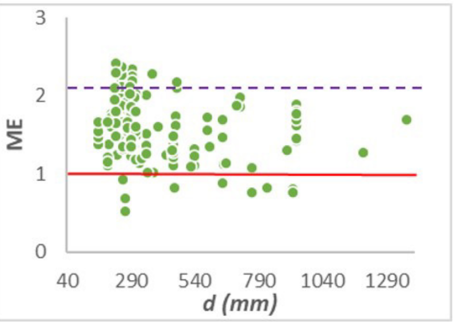

(b)

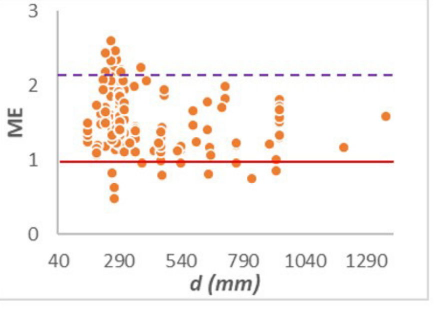

(c)

Figure 16 – ME x $d(mm)$ for beams with transverse reinforcement: ACI 318: 2019 (a), NBR 6118-14 (b), and Frosch et al. [27] (c)

As observed by Kuchma et al. [6] for the ACI 318:2014 and by Frosch et al. [27] for the unified approach, whenever a minimum reinforcement in provided, the size effect is suppressed. The same behavior occurs in the NBR 6118:2014. Nevertheless, compared to the beams without transversal reinforcement, the beams depths are limited to 1360 mm. Additionally, more studies are required to better describe how the transversal reinforcement ratio may be related to size effect suppression.

6 CONCLUSIONS

This manuscript addressed size effects in the shear strength of RC beams without transversal reinforcement. It was shown how the introduction of a size-effect factor in the formulation of NBR ABNT NBR 6118:2014 produces shear strength predictions which are more uniform with respect to longitudinal reinforcement ratio and beam depth. A new shear strength design equation was proposed for NBR 6118 that still may be calibrated to exhibit adequate reliability index. The formulation includes a correction term for reinforcement ratio, and another correction term for beam depth. It also provided higher reliability indexes and smaller model error contribution to the failure. This analysis may be improved using more uniform data, or a statistical analysis that considers the heterogeneity of data. The beam depth correction term is based on the transition between plastic and linear elastic behavior, as identified by Bažant. The notorious suppression of size effects by transversal reinforcement was also identified. Further studies are needed aiming to describe how the transversal reinforcement changes transitional dimension and suppresses size effects as effective depth increases.

REFERENCES

[1] American Concrete Institute, *Building Code Requirements for Structural Concrete*. Farmington Hills, MI, USA: Amer. Concrete Inst., 2019.

[2] Z. P. Bažant and B. H. Oh, “Crack band theory for fracture of concrete,” *Mater. Constr.*, vol. 16, pp. 155–177, 1983.

[3] Z. P. Bažant, Q. Yu, W. Gerstle, J. Hanson, and J. W. Ju, "Justification of ACI 446 proposal for updating ACI code provisions for shear design of reinforced concrete beams," *ACI Struct. J.*, vol. 105, no. 4, pp. 512–515, 2008.

[4] Q. Yu, J. L. Le, M. H. Hubler, R. Wendner, and G. Cusat, "P. Bažant, “Comparison of main models for size effect on shear strength of reinforced and prestressed concrete beams," *Struct. Concr.*, vol. 17, no. 5, pp. 778–789, 2016.

[5] M. P. Collins, P. T. Quach, and E. C. Bentz, “Shear behavior of thick slabs,” *ACI Struct. J.*, vol. 117, no. 4, pp. 115–126, 2020.

[6] D. A. Kuchma, S. Wei, D. H. Sanders, A. Belarbi, and L. C. Novak, "Development of the one-way shear design provisions of ACI 318-19 for reinforced concrete," *ACI Struct. J.*, vol. 116, no. 4, pp. 285–296, 2019.

[7] American Concrete Institute, *Building Code Requirements for Structural Concrete*. Farmington Hills, MI, USA: Ame. Concrete Inst., 2014.

[8] Associação Brasileira de Normas Técnicas, *Projeto de Estruturas de Concreto: Procedimentos*, NBR 6118:2014, 2014.

[9] R. Wendner, A. Strauss, and D. Novák, “The role of fracture mechanics in reliability analyses,” in *SP-300: Fracture Mechanics Applications in Concrete*, C. Gaedicke, Ed., Farmington Hills, MI, USA: Amer. Concrete Instit., 2015, pp 117–142.

[10] A. M. Hillerborg, P. Modéer, and P. E. Petersson, “Analysis of crack formation and crack growth in concrete by means of fracture mechanics and finite elements,” *Cement Concr. Res.*, vol. 6, no. 6, pp. 773–781, 1976.

[11] J. Planas, B. Sanz, and J. M. Sancho, “Vectorial stress-separation laws for cohesive cracking : in concrete and other quasibrittle materials,” *Int. J. Fract.*, vol. 223, no. 1, pp. 77–92, 2020.

[12] C. G. Hoover and Z. P. Bažant, "J. V., R. Wendner and M. H. Hubler, “Comprehensive concrete fracture tests: description and results," *Eng. Fract. Mech.*, vol. 114, pp. 92–103, Dec 2013.

[13] Z. P. Bažant, M. Rasoolinejad, A. Dönmez, and W. Luo, "Dependence of fracture size effect and projectile penetration on fiber content of FRC," *IOP Conf. Series Mater. Sci. Eng.*, vol. 596, no. 1, pp. 012001, 2019.

[14] C. Carloni, G. Cusatis, M. Salviato, J. L. Le, C. G. Hoover, and Z. P. Bažant, "Critical comparison of the boundary effect model with cohesive crack model and size effect law," *Eng. Fract. Mech.*, vol. 215, pp. 193–210, May 2019.

[15] J. Le, C. G. Hoover, and Z. P. Bažant, “Problems with Hu-Duan boundary effect model and its comparison to size-shape effect law for quasi-brittle fracture,” *J. Eng. Mech.*, vol. 136, no. 1, pp. 40–50, Jun 2010.

[16] C. G. Hoover and Z. P. Bažant, “Cohesive crack, size effect, crack band and work of fracture compared to comprehensive concrete fracture tests,” *Int. J. Fract. Mech.*, vol. 187, pp. 133–143, 2014.

[17] Associação Brasileira de Normas Técnicas, *Concretos para fins estruturais*, NBR 8953:2015, 2015.

[18] Canadian Standard Association, *Design of Concrete Structures*, CAN3 A23.3-94, 2014.

[19] G. N. Kani, “The riddle of shear failure and its solution,” *ACI J. Proc.*, vol. 61, no. 4, pp. 441–468, 1964.

[20] M. Iguro, T. Shioya, Y. Nojiri and H. Akiyama, “Experimental studies on shear strength of large reinforced,” *Concr. Libr. JSCE*, vol. 1, no. 345, pp. 137–154, 1984.

[21] B. A. Podgorniak-Stanik, “The influence of concrete strength distribution of longitudinal reinforcement amount,” Master thesis, Grad. Dept. Civil Eng., Toronto Univ., Toronto, Canada, 1998.

[22] P. Quach, “Understanding and safely predicting the shear response of large-scale reinforced concrete structures,” Master thesis, Dept. Civil Eng., Toronto Univ., Toronto, Canada, 2016.

[23] A. Agarwal, S. J. Foster, and M. G. Stewart, "Model error and reliability of reinforced concrete beams in shear designed according to the Modified Compression Field Theory," *Struct. Concr.*, vol. 22, pp. 3711–3726, 2021.

[24] S. J. Foster et al., “Calibration of Australian Standard AS3600 concrete structures: part I statistical analysis of material properties and model error,” *Aust. J. Struct. Eng.*, vol. 17, no. 4, pp. 242–253, 2016.

[25] S. Foster et al., *A Re-Evaluation of the Safety and Reliability Indices for Reinforced Concrete Structures Designed to AS3600: UNICIV Report R-464*. Sydney, Australia: Univ. New South Wales, 2015.

[26] I. J. S. Ribeiro, J. R. C. Pessoa, and T. N. Bittencourt, “Analysis of shear strength of complementary mechanisms "trends in reinforced concrete beams,” *Rev. IBRACON Estrut. Mater.*, vol. 16, no. 2, pp. e16208, 2023.

[27] R. J. Frosch, Q. Yu, G. Cusatis, and Z. P. Bažant, "A unified approach to design," *Concr. Int.*, vol. 1, no. 582, pp. 147–158, 2017.

[28] K. H. Reineck, E. C. Bentz, B. Fitik, D. A. Kuchma, and O. Bayrak, “ACI-DAfStb database of shear tests on slender reinforced concrete beams without stirrups,” *ACI Struct. J.*, vol. 110, no. 5, pp. 867–948, 2013.

[29] Q. Yu and Z. P. Bažant, “Can stirrups suppress size effect on shear strength of RC beams,” *J. Struct. Eng.*, vol. 137, no. 5, pp. 607–617, 2011.

[30] K. H. Reineck, E. C. Bentz, B. Fitik, D. A. Kuchma, and O. Bayrak, “ACI-DAfStb database of shear tests on slender reinforced concrete beams with stirrups,” *ACI Struct. J.*, vol. 110, no. 5, pp. 1, 2014.

[31] Fédération Internationale du Béton, *Fib Model Code for Concrete Structures 2010*. Lausanne, Switzerland: FIB, 2013.

[32] A. T. Beck, W. L. A. Oliveira, S. Nardim, and A. L. H. C. ElDebs, "Reliability-based evaluation of design code provisions for circular concrete-filled steel columns," *Eng. Struct.*, vol. 31, pp. 2299–2308, 2009.

[33] V. P. de Barros, A. T. Beck, and T. N. Bittencout, "Shear failure in reinforced concrete members without transverse reinforcement: analysis of model error of NBR6118:2014," *Rev. IBRACON Estrut. Mater.*, vol. 14, no. 1, pp. e14112, 2021.

[34] Joint Committee on Structural Safety. "JCSS probabilistic model code – part 2: load models." JCSS-LC.org. https://www.jcss-lc.org/jcss-probabilistic-model-code/ (accessed Mar. 25, 2022).

[35] W. C. Santiago and H. Machado, "S. Hampshire S., F. R. Stucchi and A. T. Beck. "Reliability-based calibration of main Brazilian structural design codes," *Lat. Am. J. Solids Struct.*, vol. 17, no. 1, pp. e245, 2020.

[36] L. G. L. Costa, W. C. Santiago, and A. T. Beck, "Probabilistic models for live loads in buildings: critical review, comparison to Brazilian design standards and calibration of partial safety factors," *Rev. IBRACON Estrut. Mater.*, vol. 16, no. 2, pp. e16204, 2023.

[37] A. T. Beck and A. C. Souza Jr., "A first attempt toward a reliability-based calibration of Brazilian structural design codes," *J. Braz. Soc. Mech. Sci. Eng.*, vol. 32, pp. 119–127, 2010.

Author contributions: IJSR: conceptualization, data curation, formal analysis, writing, methodology; JRCP: supervision, writing, methodology; TNB: conceptualization, data curation, formal analysis, writing, methodology; ATB: conceptualization, data curation, formal analysis, writing, methodology.

Editors: Leandro Trautwein, Mauro Real, Mario Pimentel.

Annex A. DATA FOR CONCRETE BEAMS WITH STIRRUPS

Ahmad, S.H.; Park, F.; El-Dash, K. (1995): Web reinforcement effects on shear capacity of reinforced high-strength concrete beams. Magazine of Concrete Research 47 (Sep.1995), No. 172, 227-233

Ahmad, S.H.; Xie, Y.; Yu, T.(1996): Effectiveness of Shear Reinforcement for Normal and High-Strength Concrete Beams. Structural Engineering Review, V.8 (1996), No.1, 65-78

Angelakos, D.; Bentz, E.C (2001): Collins, M.P.: Effect of concrete strength and minimum stirrups on shear strength of large members. ACI Structural Journal 98 (2001), Title 98-S28, May-June, 290 - 300

Aparicio, A.; Calavera, J.; del Pozo, F.J. (1997): Testing strut compression shear failure in beams. Polytechnic University of Madrid, 1997. pp. 55 [see also: Gettu et al (1997); Rozas Hernando et al. (1997)]

Bernhardt, C.J.; Fynboe, C.C. (1986): High strength concrete beams. Nordic Concrete Research, Norske Betongforening, Oslo 1986

Bhal, N.S. (1968): Über den Einfluß der Balkenhöhe auf die Schubtragfähigkeit von einfeldrigen Stahlbetonbalken mit und ohne Schubbewehrung. Otto-Graf-Institut, H.35, Stuttgart, 1968

Bræstrup, M.W.; Nielsen, M.P.; Bach, F.; Jensen, B. Chr. (1976): Shear Tests on Reinforced Concrete T-Beams. Series T. Structural Research Laboratory, Technical University of Denmark, rappor Nr.R 72,1976

Cladera, A.; Marí, A.R. (2002): Shear Strength of Reinforced High –Strength and Normal –Strength Concrete Beams. A New Smiplified Shear Design Method. Universitat Politécnica de Catalunya, 1-19, 2002

Cederwall, K.; Hedman, O.; Losberg, A. (1974): Shear strength of partially prestressed beams with pretensioned reinforcement of high grade deformed bars. SP 42 – 9

Gabrielsson, H. (1993): High Performance Concrete Beams Tested in Shear. Comparison between the Traditional Approach and the Modified Compression Field Theory. 169-176 in: Holand, I.; Sellevold, E. (Editors): 'Utilization of High Strength Concrete', 3rd Symp. in Lillehammer, Norway, 20.-23. June 1993, Proc. V.1. Norwegian Concrete Assoc., Oslo 1993. ISBN 82-91341-00-1

Guido, C. C.; Radogna E. F. (1963): Contributo teorico sperimentale allo studio della precompressione parziale. Giomate del Precompresso. Venezia (Okt. 1963)

Hamadi, Y.D. (1976): Force transfer across cracks in concrete structures. PhD-thesis, Polytechnic of Central London, 1976

Hegger, J.; Görtz, S; Will, N.; Drössler, C.; Tigges, C. (2001): Tragfähigkeit von Bauteilen aus selbstverdichtendem Beton. BuStb 96 (2001), H. 11, 691-697

Hegger, J.; Görtz, S. (2003): Analyse des Schubrissverhaltens und dessen Auswirkungen auf die Querkrafttragfähigkeit. RWTH Aachen, Institut für Massivbau, Schlussbericht DBV 227, Institutsbericht-Nr. 86/2003, Aachen, September 2003Hegger, J.; Görtz, S.; Neuser, J.U. (1999): Hochfester Beton für Spannbetonbalken mit sofortigem Verbund. Schlußbricht (DBVNr.192), Institutsbericht Nr. 55/99, RWTH Aachen, 1999

Kautsch, R. (2010): Beitrag zur Nachweisführung von querkraftbewehrten Stahlbeton- und Spannbetonquerschnitten unter kombinierter Biege- und Schubbeanspruchung auf Grundlage der erweiterten technischen Biegelehre. (Analysis of shear reinforced r.c.- and p.c.-crosssections subjected to combined bending and shear on basis of the extended bending theory). Diss. Fachbereich Architektur / Raum- und Umweltplanung / Bauingenieurwesen der TU Kaiserslautern. D 386, Kaiserslautern 2010. pp. 251

Kong, F.-K.; Robins, P.J.; Cole, D.P. (1970): Web Reinforcement Effects on Deep Beams. ACI-Journ. V.67 (1970), No.12, Dec., 1010-1017

Leonhardt, F.; Walther, R. (1962b): Versuche an Plattenbalken mit hoher Schubbeanspruchung. DAfStb H.152, Beuth Verlag Berlin, 1962

Leonhardt, F.; Walther, R. (1962c): Versuche an schlaff bewehrten Rechteck- und Plattenbalken mit Schubbewehrung; 1. Teil; Forschungsreihe über die Tragfähigkeit auf Schub von Stahl- und Spannbetonbalken, FMPA (Otto-Graf-Institut), Stuttgart, März 1962

Leonhardt, F.; Walther, R. (1962d): Versuche an schlaff bewehrten Rechteckbalken und Platten ohne Schubbewehrung; 2. Teil; Forschungsreihe über die Tragfähigkeit auf Schub von Stahl- und Spannbetonbalken, FMPA (Otto-Graf-Institut), Stuttgart, März 1962

Leonhardt, F., Walther, R. (1962e): Versuche an schlaff bewehrten Rechteckbalken und Platten ohne Schubbewehrung; Zusammenfassung und vorläufige Schlußfolgerungen; Forschungsreihe über die Tragfähigkeit auf Schub von Stahl- und Spannbetonbalken, FMPA (Otto-Graf-Institut), Stuttgart, April 1962 DAfStb H. 617: Report on ACI-DAfStb Shear Databases 2015 - Part 4.1: Attachment 4.2-1 4 2016

Leonhardt, F., Walther, R. (1963): Schubversuche an Plattenbalken mit unterschiedlicher Schubbewehrung. DAfStb H.156, Beuth Verlag, Berlin, 1963

Levi, F.; Marro, P. (1989): Shear Tests up to Failure of Beams made waith Normal and High Strength Concrete. p. 11-24 in: CEB-Bulletin No.193 (1989)

Levi, F.; Marro, P. (1993): Shear Tests on HSC Prestressed Beams - Proposals of new Interpretative Models. High-Strength Concrete (1993), Proceedings V.1, 293-305

Maruyama, K.; Rizkalla, S.H. (1988): Shear design consideration for pretesioned prestressed beams. ACI-Journ. V.85 (1988), No.5, Sep.-Oct., 492-498

Moayer, M.; Regan, P.E. (1974): Shear strength of prestressed and reinforced concrete T-beams. 183-214 in: Shear in reinforced concrete. Vol. 1, Publ. SP 42, ACI Detroit. 1974

Özden, K. (1967): An Experimental Investigation on the Shear Strength of Reinforced Concrete Beams. Structural Research Laboratory (1967), Technical University of Denmark

Ozcebe, G.; Ersoy, U.; Tankut, T. (1999): Evalution of minimum shear reinforcement requirements for higher strength concrete. ACI Struct. Journ. V.96 (1999), No. 3, May-June

Petersson, T. (1972): Shear and Torsion in reinforced concrete beams. National Swedish Building Research, Document D10:1972

Quast, U. (1999): Einfluß von Langzeitwirkungen auf den Neigungswinkel von Schubrissen. Schlußbericht zum Forschungsvorhaben QU 48/5-1. Arbeitsbereich Massivbau, Technische Universität Hamburg-Harburg (TUHH), 31.03. 1999. pp. 36 + 121 Anlagen DAfStb H. 617: Report on ACI DAfStb Shear Databases 2015 - Part 4.1: Attachment 4.2-1 5, 2016

Reineck, K.-H.; Wohlfahrt, R.; Hardjasaputra, H. (2001): Verformungsverhalten und Tragfähigkeit dünner Stege von Stahlbeton-und Spannbetonträgern mit hoher Betongüte (Deformations and strength of thin webs of reinforced and prestressed high strength concrete beams). DafStb-Heft 517, Beuth Verlag, Berlin 2001

Roller, J.J., Russel, H.G. (1990): Shear Strength of High-Strength Concrete Beams with Web Reinforcement. ACIJourn. V.87, N. 2, (1990), March-April, 191-198

Rosenbusch, J.; Teutsch, M. (2002): Trial Beams in Shear. Brite/Euram project 97-4163, Final Report Sub task 4.2, Institut für Baustoffe, Massivbau und Brandschutz, TU Braunschweig, January, 2002

Rosenbusch, J. (2003): Zur Querkrafttragfähigkeit von Balken aus stahlfaserverstärkten Stahlbeton. Diss., Fachbereich Bauingenieurwesen, Technische Universität Carolo-Wilhelmina zu Braunschweig, Juni 2003. pp. 199

Sarsam, K.F.; Al-Musawi, J.M.S. (1992): Shear Design of High-and Normal Strength Concrete beams with Web Reinforcement. ACI-Journ. V.89 (1992), No.6, Nov.-Dec., 658-664

Soerensen, H.C. (1974): Shear Test on 12 Reinforced Concrete T-Beams. Structural Research Laboratory (1974), Rapport Nr. R 60, Technical University of Denmark Stroband, J. (1997): Shear Capacity of High-Strength Concrete Beams with Shear Reinforcement. Progress in Concrete, V.5 (1997), TU Delft, 87-96 Sunderland, A. (1947): Shear strength of reinforced concrete rectangular and T-beams, Ph. D. Thesis, University of Leeds (1947)

Tan, K.-H.; Kong, F.-K.; Teng, S.; Weng, L.-W. (1997): Effect of web reinforcement on high-strength concrete deep beams. ACI Structural Journal, V. 94, No. 5, Sep.-Oct. 1997, 572-582

Tan, K.-H.; Kong, F.-K.; Teng, S.; Guan, L. (1995): High-strength concrete deep beams with effective span and shear span variations. ACI Structural Journal, V. 92, N. 4, July-Aug. 1995, 395-405

Tan, K.; Teng, S.; Kong, F.-K.; Lu, H. (1997): Main Tension Steel in High Strength Concrete Deep and Short Beams. ACI Structural Journal, November- December 1997, 752- 768

Yoon, Y.-S.; Cook, W.D.; Mitchell, D. (1996): Minimum Shear Reinforcement in Normal, Medium and HighStrength Conc rete Beams. ACI-Journ., V.93 (1996), No.5, Sept.-Oct., 576-584

Yoshida, Y. (2000): Shear Reinforcement for Large, Lightly Reinforced Concrete Members. Master Thesis, Grad.Dep. of Civil Eng., University of Toronto (2000)